Theoretical and Experimental Analysis of Group Piles of Jet and Concrete Columns using the Double Grouting Technique Subjected to Axial Loading on Sandy Soil

Rana M. Al-Khadaar
Department of Civil Engineering, University of Baghdad, Iraq
ranaal-khadaar@coeng.uobaghdad.edu.iq (corresponding author)

Mahmood D. Ahmed
Department of Civil Engineering, University of Baghdad, Iraq
dr.mahmood.d.a@coeng.uobaghdad.edu.iq

Received: 24 March 2024 | Revised: 5 April 2024 | Accepted: 11 April 2024

ABSTRACT

This research deals with modifying improvement techniques by using a new technology depending on the properties of the subsoil and the surrounding soil. Jet grouting is one of these techniques utilized instead of normal deep foundations, such as piles, peers, and raft foundations, because it increases the bearing capacity, reduces the settlement, and decreases permeability. In this research, the effect of double-pile and (2*2) jet column piles was studied in the laboratory by employing a jet grouting machine for sand soil, and the results were compared with those of similarly distributed concrete piles. Moreover, the two groups were theoretically analyzed with the 3D ABAQUS finite element software. It was found that with the jet pile, the applied load is greater and the settlement is smaller than that with the concrete pile. The ultimate pile ratio obtained through laboratory tests in the (2*1) jet pile and the concrete pile groups was 71.2% and 75%, respectively. The settlement ranged from 0.00135 to 0.00148 m with the jet pile and ranged from 0.034 to 0.035 m with the concrete pile.

Keywords-3D finite element analysis; jet grouting column; concrete pile column; sandy soil; elastoplastic model; axial load; settlement; stress

I. INTRODUCTION AND LITERATURE REVIEW

Some large-scale pile load tests used in previous works and the followed load-deformation methods are mentioned below:

- The behavior of compression piles and axial loading was studied in [1].
- The behavior of cemented sand in Kuwait under axial load on a single board pile with tension and compression and the application of compression load on pile groups were examined in [2]. The group efficiency ranged from 1.22 to 1.93 depending upon the spacing of the pile group.
- The interaction among the bored pile, the cap pile, and the surrounding soil under axial compression load by using a 3D elastoplastic Finite Element (FE) software was explored in [3]. It was concluded that the increase in length-to-depth ratio causes a decrease in pile cap-bearing pressure, and the increase in tip-bearing pressure causes an raise in the relative stiffness of the soil elastic modulus to pile elastic modulus [3].
- The behavior of aluminum pile groups of straight edge and enlarged (belled) pile groups by applying an axial load in the laboratory in a brick masonry tank with different diameters was investigated in [4]. It was found that the load carrying capacity increased by about 40% in a belled pile model with a decrease in the length-to-depth ratio.
- The effect of the efficiency factor on a single installed pile was reviewed in [5], along with group testing regarding spacing, soil parameters, and soil-pile friction [5].
- The behavior of steel pipe piles and pile groups in sandy soils was studied in [6]. Tests were conducted in the laboratory under a controlled density of dry clean uniform sand and by using the axial load settlement characteristic of rectangular, circular, and square pile groups [6].
- The behavior of concrete piles of the (4*4) group with caps of different lengths and the effect of vertical or lateral loading and spacing on the bearing capacity of soil by using 3D and 2D Plaxis were the discussion subject of [7].

- The vertical effective stress to reduce the differential settlement between the two piles by utilizing a 3D coupled consolidation FE program with a hypoplastic model in saturated non-uniform silty clay was studied in [8].
- The effect of a 6 m tunnel on a (2*2) pile group in saturated stiff clay by employing a 3D elastoplastic and a coupled consolidated FE with different factors was investigated in [9].

Using jet piles instead of other pile types constitutes an improvement that helps in the support of the deep foundation. Jet grouting, which is a modified technology compared to other grouting techniques, has been implemented in difficult situations, confined and unconfined areas, and saturated and unsaturated lands. Authors in [10] studied the deployment of jet grouting in the Runway End safety area, which is a part of the International Sydney Airport, with the purpose of increasing ground bearing and create impermeable barriers to cut off the water flow during construction. The design was supported by the FE software PLAXIS. Authors in [11] explored the usage of the double jet grouting technique to stabilize cohesionless soils for the York Durham Sewage System along with a slurry wall. It was found that the unconfined compressive strength ranged from 4.6 to 9.7 MPa after 28 days. Authors in [12] discussed the parameters that affect the soil of Shahriar dam, namely the diameter of jet columns, soil uniaxial compressive strength, amount of water used with cement, amount of grout, amount of air pressure, lifting speed, and rotation speed. Authors in [13] used experimental data and numerical analysis to determine the load settlement response of axially loaded jet grouting columns. It was found that jet grouting columns were able to sustain an axial load 20 to 30% greater than the expected load for a bored pile of similar dimensions. Authors in [14] collected experimental information from the field and analyzed it to derive a simple expression for the average diameter of the jet grouted columns in terms of different parameters, such as injection system, soil type or gradation, and injected-fluid composition. Authors in [15] gathered data from a field prototype of single and double bored piles with a length to depth ratio of 13.3 and spacing equal to 3 times the diameter and subjected to axial vertical load in soft clay in South Iraq. The results were compared with those obtained from a theoretical analysis Authors in [16] focused on the strength of the material to be used with single and double jet grouting in sandy and clayey soils. It was discovered that the cement-to-soil ratio raised the uniaxial compressive strength. Furthermore, it was found that the injection system and material strength are closely related. Authors in [17] collected data on jet grouting to predict the diameter of jet columns for different types of jet grouting and followed the Bayesian method with statistic calculations to predict the size of the jet grouting columns. Authors in [18] presented a historical review for different types of jet grouting techniques for different types of soils.

II. MATERIALS AND METHODS

A. Soil

The experimental part of the current research was conducted in the Laboratory of Soil Mechanics in the Civil Engineering Department, College of Engineering, University of Baghdad, Iraq. The soil used in the investigation was taken from the Al-Rashdia site in the south of Baghdad. The soil was SP, consisting of 98.36% sand and 1.64% silt and clay [19] with a specific gravity equal to 2.67 [20]. The angle of internal friction φ was 34.56° and the cohesion C was 8 kN/m² [21].

A square steel tank was engaged, with dimensions equal to 1.2*1.2*1.2 m, along with a frame to hold the mechanical jack that was employed to apply the vertical axial load, as portrayed in Figure 1. The raining steel tank hanging in the frame helps distribute the soil with the same relative density. The scaling factor utilized is (1/20), which is enough for this occasion.

B. Concrete Pile Columns

The mixture deployed in the experimental study consisted of sand, gravel, cement, water, superplasticizer, and polyvinyl alcohol (PVA). The sand utilized conformed to IQS No. 45 [24]. The cement used in the mix was sulfate-resisting cement C3A, which is recommended for foundation works. A steel pipe pile 0.5 m long and with a diameter of 0.0572 m was put into service to form the concrete pile. The average compressive strength of the mixture was 33700 kN/m² [22].

Fig. 1. Steel tank model with a mechanical jack.

TABLE I. PHYSICAL AND MECHANICAL PROPERTIES OF THE JET GROUTED COLUMN CORE

Unit weight (kN/m³)	16.264-22.814
Modulus of Elasticity (kN/m²)	412062-15490250
Split tensile strength (kN/m²)	1599-39460
Uniaxial compressive strength (kN/m²)	11200-1411000
Cohesion (kN/m²)	2090-117981
Angle of internal friction (degrees)	49°-71°

C. Jet Grouting Column

A modified jet grouting machine manufactured by the researchers was deployed to work as a double jet grouting machine to inject and formulate a jet grouting pile in the steel tank. The injected material contained 1:1 water to cement ratio. After the process of injection, curing was accomplished by covering the grouted space with a canvas wet cover. The ranges of the physical and mechanical properties of the jet grouting material are displayed in Table I.

III. THE NUMERICAL METHOD

Finite Element (FE) analysis is a process that allows simulating the behavior of parts and assembling those parts with suitable boundary conditions and time steps for every case. The ABAQUS FE software was implemented to compare the theoretical results with those obtained from the laboratory. The element model is a brick element of 8 nodes, which can be expressed in a C3D8R Linear Hexagonal reduced integration, or an 8-node brick element reduced integration with hourglass control stiffness, which defines the elasticity of the material. Boundary conditions should be applied in the program for the latter to be defined by selecting faces or reference nodes to know the reaction or moment. The degrees of freedom should be specified in the model, whether double or (2*2) pile. The bottom face is selected not to move in the X, Y, and Z directions, whereasd the sides of the model are fixed in the X and Z directions and allowed to move in the Y direction only. The FE mesh after assembling the physical model was used for the soil, pile, and pile cap parts. There are coarse and fine types of mesh, the choice depends upon the selected time step and the accuracy of the results. The best element size that suits the model and is compatible with the time step is chosen. Due to the inhomogeneity and anisotropy of the material and since the soil is a complicated material, the Mohr-Coulomb theory was adopted to model the plasticity yield criteria. This model is based upon plotting Mohr's circle for the condition of stress at failure in the primary maximum and minimum stress planes. The main parameters needed for this model are cohesion C, angle of internal friction φ, and dilatancy angle ψ. In elastic models for pile and cap pile, additional parameters are needed, namely the modulus of elasticity E, and Poisson's ratio ν.

IV. THE MODELING PROBLEM

As stated above, the laboratory model was a steel box of dimensions 1.2*1.2*1.2 m. To accomplish workability, the Z direction or depth of soil was set equal to 0.8 m instead of 1.2 m. The same material properties of soil, jet column, concrete pile, and pile cap were used in the analysis performed by the ABAQUS. Figure 2(a) manifests sketches of the 3D model for a (2*1) pile whether it is a jet pile, concrete pile, or pile cap, whose dimensions are 0.27 *0.10 m, and the soil model. Figure 3(b) shows the same dimensions for the jet column pile, pile cap, and soil model with different length to diameter (L/D) ratios. For the (2*2) 3D pile, the FE mesh has the same material properties as in Table II with pile cap dimensions 0.27*0.27 m. Also, the same (L/D) ratio was deployed in the (2*2) model of piles, pile cap, and soil. Both (2*1) and (2*2) models are subjected to axial load by a mechanical jack until failure occurs. The values of (L/D) were 15, 25, and 30. The diameter of the pile was held constant; thus, the lengths of the pile were 0.90, 1.5, and 1.70 m. The same ratio was utilized for the (2*1) and (2*2) groups.

TABLE II. MATERIAL PROPERTIES USED IN ABAQUS

	Concrete pile	Jet pile	Soil
Modulus of elasticity (kN/m^2)	30*10^6	70*10^6	30000
Unit weight (kN/m^3)	24	19.529	14.32
Poisson's ratio	0.2	0.2	0.3
Length (m)	0.45	0.45	------
Cohesion (kN/m^2)	-------	-------	8
Angle of internal friction	-------	-------	34.56
Dilatancy angle	------	------	4.56
Diameter (m)	0.0572	0.0572	------

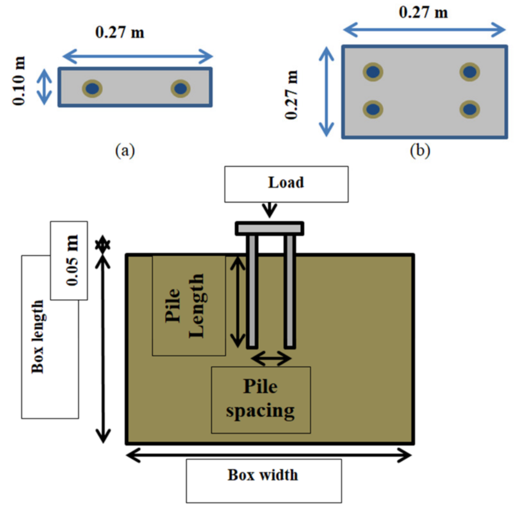

Fig. 2. Model sketch of (a) (2*1) group and (b) (2*2) group used in ABAQUS.

V. RESULTS AND DISCUSSION

The values of load-bearing capacity were obtained from laboratory tests by engaging a steel model for the (2*1) group for the concrete pile and by using a jet grouting machine and injecting the column. The values of the applied load were read by the load cell and the displacements were read by the Linear Variable Differential Transformer (LVDT). Curing over the load was applied by a mechanical jack and the load settlement curve was determined, according to [23]. From Figure 3, it can be noted that the ultimate load pile ratio for the concrete pile was 75%, whereas for the jet pile, it was 71.2%.

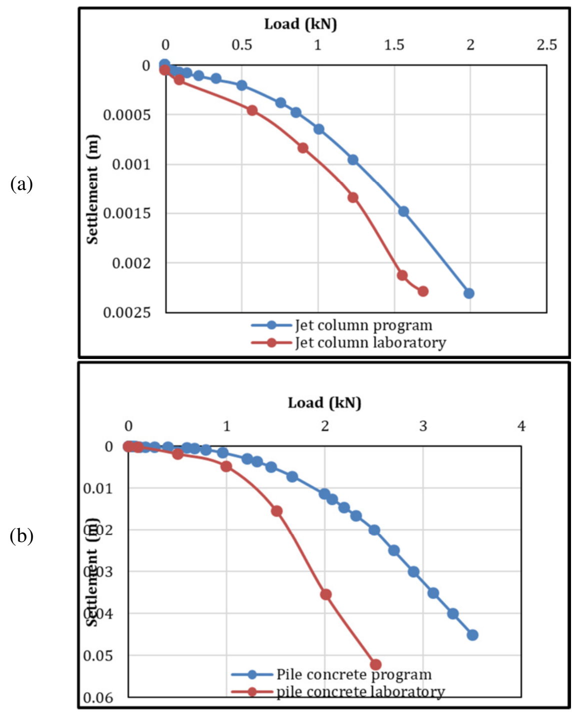

Fig. 3. Comparison between laboratory and ABAQUS (a) concrete pile and (b) jet pile column.

The load settlement curves for a concrete pile, depicted in Figure 4, for different (*L*/*D*) values coincide with each other for pile lengths equal to 0.9 and 1.5 m, but for a pile length of 1.7 m the curve deviates from the others. Such deviation may be attributed to the interaction in ABAQUS, which may have a little effect. Also, the end bearing effect is more predominant than the side friction but this effect disappears in large scales. Figure 5 portrays the load settlement curves for the jet grouting column and a similar phenomenon as in Figure 4 appears where the curves for pile lengths of 1.5 and 1.7 coincide while the curve for the pile length of 0.9 m deviates. Figure 6 showcases the variation of stress along the pile length, which is greater for the jet pile than for the concrete pile, but in a small range if compared with the settlement. Figure 7 demonstrates the variation of settlement along the pile length, which is less in the jet grouting column than in the concrete pile column. Figure 8 provides a comparison between the load settlement curves for concrete and jet piles for the (2*2) group pile. It is clear that the jet pile can carry a load of 3.5 kN, whereas the load that a concrete pile can carry is only 2 kN. However, the settlement accompanying the jet pile is 0.008 m, whereas with the concrete pile, it is 0.0125 m. This phenomenon expresses the reason why jet grouting is a very effective method to improve soil. Furthermore, Figure 9 indicates that the settlement in the jet grout column is reduced in comparison with the concrete pile, whereas the stress in the jet pile is increased in comparison with the concrete pile. Figure 10 presents the load settlement curve for the (2*2) group pile for different (*L*/*D*) values. As the length of the jet pile increases, the bearing load increases while the settlement of pile decreases. From Figures 11 and 12, it can be seen that the values of stress increase for the jet column more than for the concrete column along the interaction point between soil and pile, whereas the settlement decreased.

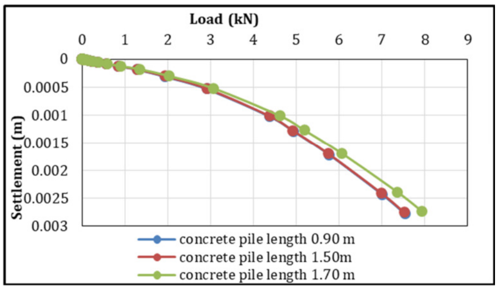

Fig. 4. Load settlement curve for different (*L*/*D*) values of the (2*1) group of concrete pile model.

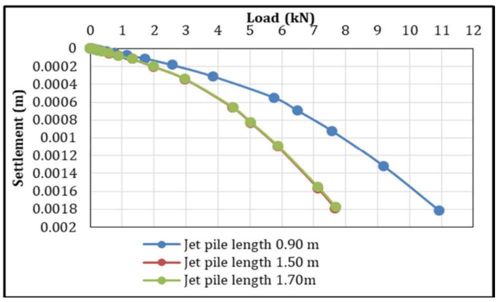

Fig. 5. Load settlement curve for different (*L*/*D*) values of the (2*1) group of jet pile model.

(a)

(b)

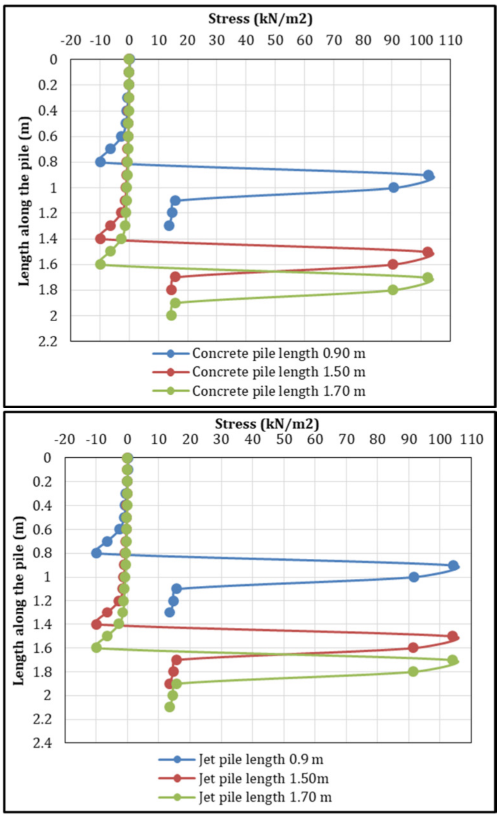

Fig. 6. Variation of stress along the interaction for different (*L*/*D*) values between soil and (a) concrete pile, (b) jet pile column.

(a)

(b)

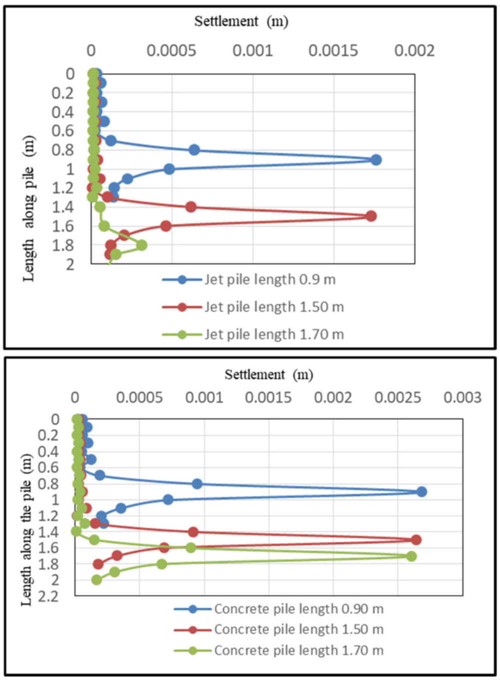

Fig. 7. Settlement along the interaction for different (*L*/*D*) values between soil and (a) jet pile column, (b) concrete pile column.

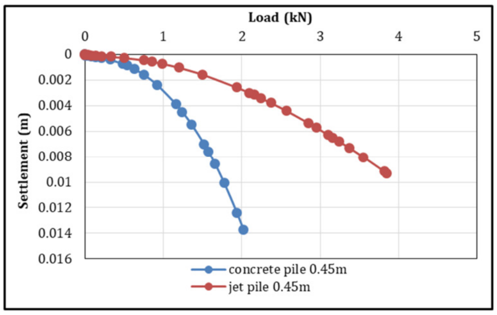

Fig. 8. Comparison of the load settlement curves of concrete pile column and jet column for the (2*2) group.

(a)

(b)

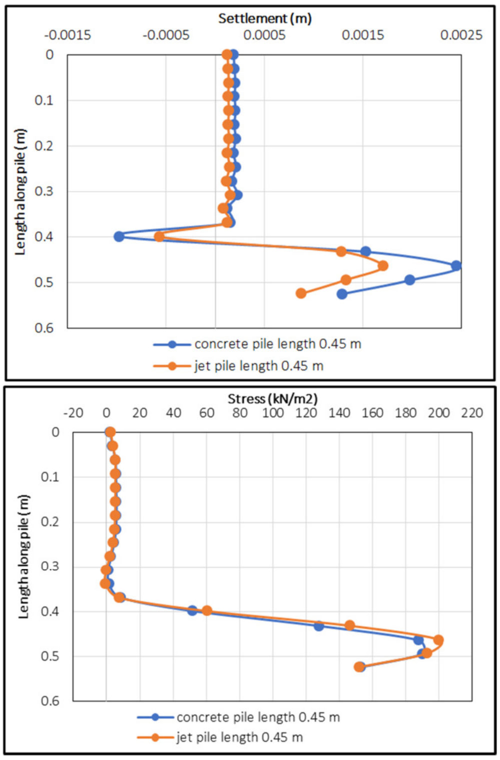

Fig. 9. (a) Comparison of settlement along the interaction between soil, concrete pile, and jet column, (b) comparison of stress along the interaction between soil, concrete pile, and jet column, for group (2*2).

(a)

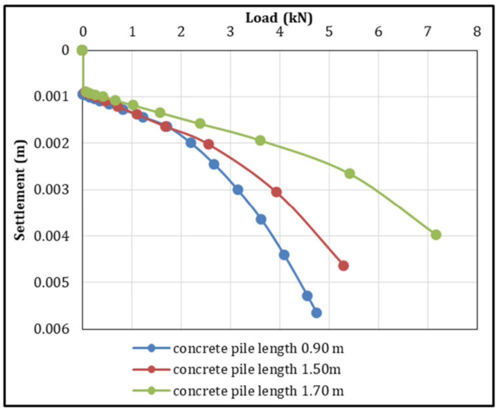

(b)

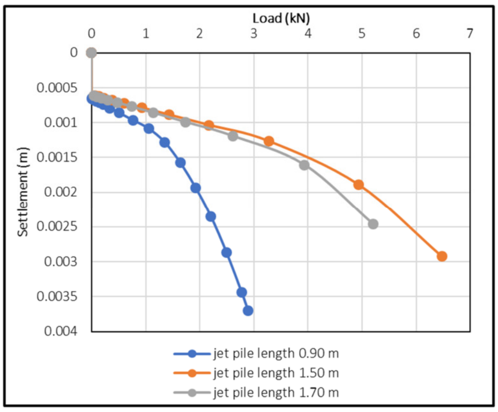

Fig. 10. Load settlement curve for different (*L*/*D*) ratios of: (a) (2*2) concrete pile group, (b) (2*2) jet column pile group.

(a)

(b)

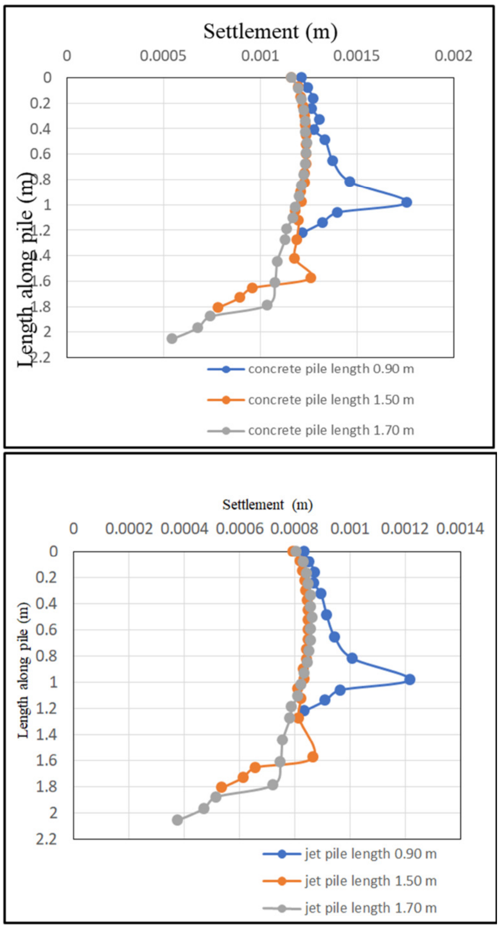

Fig. 11. Comparison of settlement along the interaction between: (a) soil and concrete (2*2) pile group, (b) soil and jet (2*2) pile group.

(a)

(b)

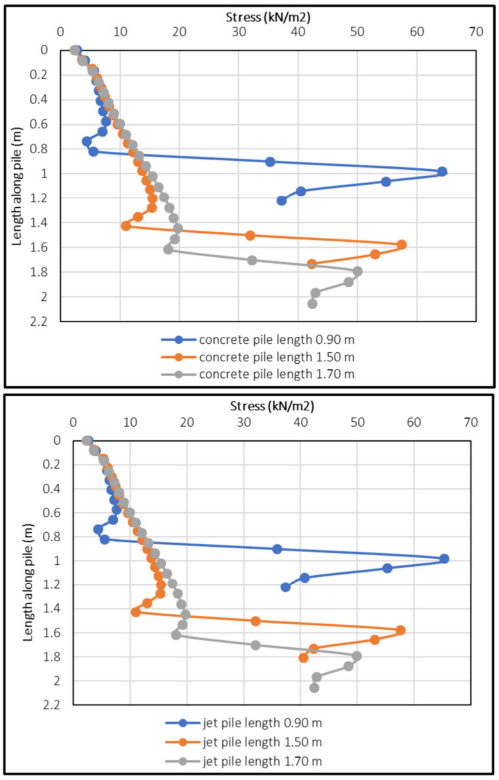

Fig. 12. Comparison of stress along the interaction between: (a) soil and concrete pile group (2*2) and (b) soil and (2*2) jet pile group.

VI. CONCLUSIONS

This research focused on soil improvement by following the double jet grouting technique. A laboratory grouting machine was used to experiment with a (2*1) group of piles at first by employing a concrete pile with a cap and next by utilizing a jet grouting column. The results from the laboratory were compared with the numerical values obtained with the use of the finite element software ABAQUS for both types, concrete and jet, columns. Laboratory experiments were also conducted for a (2*2) group of piles with cap pile and the results were compared with the theoretical values. From the findings, it was concluded that:

- Shen's method is the most appropriate one to determine the values of the applied load and settlement in order to prepare the load-settlement curves for both concrete and jet columns.
- With jet grouting, the diameter of the pile is considered the controller. For any calculations and any changes in scale, the diameter was held constant while the length was the variable.
- In a (2*1) group of piles, the percentage of ultimate load for the jet column was 71.2%, whereas for the concrete column it was 75%.
- The settlement is about 96.2% of that of the concrete pile.
- The increase in stress along the interaction of the jet pile rose by about 1.52 to 1.69%.
- Settlement ranged between 52.27 and 73% along the interaction of the jet pile in comparison with the concrete pile.
- In the (2*2) group, the increase in bearing load is about 43% when juxtaposed with the concrete pile.
- The reduction in the settlement is about 36% when compared with a concrete pile.
- For a group of four jet piles with different (*L*/*D*) ratios, a ratio of 25 gives an increase in bearing load by about 30% and a reduction in settlement by about 39% when compared with a similar group of concrete piles.

REFERENCES

[1] B. H. Fellenius, *Guidelines for the interpretation and analysis of the static loading test: a continuing education short course text*. Deep Foundations Institute, 1990.

[2] N. F. Ismael, "Axial Load Tests on Bored Piles and Pile Groups in Cemented Sands," *Journal of Geotechnical and Geoenvironmental Engineering*, vol. 127, no. 9, pp. 766–773, Sep. 2001, https://doi.org/10.1061/(ASCE)1090-0241(2001)127:9(766).

[3] F. I. Shalabi, M. U. Saleem, H. J. Qureshi, M. Arifuzzaman, K. Khan, and M. M. Rahman, "3D FE analysis of bored pile- pile cap interaction in sandy soils under axial compression- parametric study," *Journal of Engineering Research*, vol. 11, no. 4, pp. 301–313, Dec. 2023, https://doi.org/10.1016/j.jer.2023.07.004.

[4] S. Goudar and A. Kamatagi, "An Experimental Evaluation of Axial Load Bearing Capacity of Belled and Straight Piles Embedded in Sand," *International Journal of Engineering*, vol. 35, no. 8, pp. 1599–1607, Aug. 2022, https://doi.org/10.5829/ije.2022.35.08b.16.

[5] A. Norkus and V. Martinkus, "Bearing capacity and stiffness of pile group foundation," in *13th International Conference Modern Building Materials, Structures and Techniques*, Vilnius, Lithuania, Dec. 2019, https://doi.org/10.3846/mbmst.2019.135.

[6] P. K. Singh and V. K. Arora, "Behavior of Pile Groups Subjected to Vertical Loading," *International Journal of Engineering Research & Technology*, vol. 3, no. 3, pp. 2053–2057, 2014.

[7] A. Firoozfar, A. Rostami, H. Ghaderi, H. Zamani, and A. Rostamkhani, "Assessing the Effects of Length, Slope and Distance between Piles on the Bearing Capacity of a Pile Group under Axial Loading in Granular Soil," *Engineering, Technology & Applied Science Research*, vol. 7, no. 5, pp. 1894–1899, Oct. 2017, https://doi.org/10.48084/etasr.1352.

[8] M. A. Soomro, A. S. Brohi, M. A. Soomro, D. K. Bangwar, and S. A. Bhatti, "3D Numerical Modeling of Pile Group Responses to Excavation-Induced Stress Release in Silty Clay," *Engineering, Technology & Applied Science Research*, vol. 8, no. 1, pp. 2577–2584, Feb. 2018, https://doi.org/10.48084/etasr.1748.

[9] M. A. Soomro, D. K. Bangwar, M. A. Soomro, and M. A. Keerio, "3D Numerical Analysis of the Effects of an Advancing Tunnel on an Existing Loaded Pile Group," *Engineering, Technology & Applied Science Research*, vol. 8, no. 1, pp. 2520–2525, Feb. 2018, https://doi.org/10.48084/etasr.1693.

[10] B. Hamidi, M. Krzeminski, D. Berthier, P. Vincent, M. Yates, and M. Bachy, "The application of Jet Grouting for the construction of Sydney International Airport Runway End Safety Area," *Australian Geomechanics Journal*, vol. 45, no. 4, pp. 1–8, Dec. 2010.

[11] M. Chuaqui, F. Hu, N. Gurpersaud, and D. Lees, "A Case Study: Two-fluid Jet Grouting for Tunneling Application - Soil stabilization and Permeability Reduction," in *4th International Conference on Grouting and Deep Mixing*, New Orleans, LA, USA, Feb. 2012, pp. 868–879, https://doi.org/10.1061/9780784412350.0070.

[12] B. Nikbakhtan, K. Ahangari, and N. Rahmani, "Estimation of jet grouting parameters in Shahriar dam, Iran," *Mining Science and Technology*, vol. 20, no. 3, pp. 472–477, May 2010, https://doi.org/10.1016/S1674-5264(09)60228-3.

[13] G. Modoni, J. Bzowka, and J. Pieczyrak, "Experimental investigation and numerical modelling on the axial loading of jet grouting columns," *Architecture Civil Engineering Environment*, vol. 3, no. 3, pp. 69–78, 2010.

[14] A. Flora, G. Modoni, S. Lirer, and P. Croce, "The diameter of single, double and triple fluid jet grouting columns: prediction method and field trial results," *Geotechnique*, vol. 63, no. 11, pp. 934–945, Sep. 2013, https://doi.org/10.1680/geot.12.P.062.

[15] A. M. AL-Kinani and M. D. Ahmed, "Comparison of Single and Group Bored Piles Settlement Based on Field Test and Theoretical Methods," *Journal of Engineering*, vol. 26, no. 2, pp. 144–158, 2020, https://doi.org/10.31026/j.eng.2020.02.11.

[16] G. Modoni *et al.*, "Strength of sandy and clayey soils cemented with single and double fluid jet grouting," *Soils and Foundations*, vol. 59, no. 4, pp. 942–954, Aug. 2019, https://doi.org/10.1016/j.sandf.2019.03.007.

[17] L.-S. Zhao, X. Qi, F. Tan, and Y. Chen, "A new prediction model of the jet grouting column diameter for three jet grouting systems," *Computers and Geotechnics*, vol. 163, Nov. 2023, Art. no. 105753, https://doi.org/10.1016/j.compgeo.2023.105753.

[18] M. D. Ahmed and R. M. Al-Khadaar, "Review of Jet Grouting Practice around the World," *Journal of Engineering*, vol. 29, no. 7, pp. 48–70, 2023, https://doi.org/10.31026/j.eng.2023.07.04.

[19] *ASTM D422-63(2007), Standard Test Method For Particle-Size Analysis Of Soils*. West Conshohocken, PA, USA: ASTM International, 2007.

[20] ASTM Committee D-18 on Soil and Rock, *Standard test methods for specific gravity of soil solids by water pycnometer*. ASTM international, 2006.

[21] *ASTM D3080/D3080M-11(2011), Standard Test Method for Direct Shear Test of Soils Under Consolidated Drained Conditions*. West Conshohocken, PA, USA: ASTM International, 2011.

[22] *ASTM C39/C39M-21(2021), Standard Test Method for Compressive Strength of Cylindrical Concrete Specimens*. West Conshohocken, PA, USA: ASTM International, 2021.

[23] A. Mishra, V. A. Sawant, and V. B. Deshmukh, "Prediction of Pile Capacity of Socketed Piles Using Different Approaches," *Geotechnical and Geological Engineering*, vol. 37, no. 6, pp. 5219–5230, Dec. 2019, https://doi.org/10.1007/s10706-019-00976-0.

[24] *Iraqi Specification No. 45. Aggregate from Natural Sources for Concrete and Construction*. Baghdad, Iraq: Central Organization for Standardization and Quality Control, 2019.

[25] I. F. Al-Mulla, A. S. Al-Ameeri, A. S. Al-Rihimy, and T. S. Al-Attar, "Elasticity and Load-Displacement Behavior of Engineered Cementitious Composites produced with Different Polymeric Fibers," *Engineering, Technology & Applied Science Research*, vol. 14, no. 1, pp. 13026–13032, Feb. 2024, https://doi.org/10.48084/etasr.6731.

[26] B. Uzbas and A. C. Aydin, "Microstructural Analysis of Silica Fume Concrete with Scanning Electron Microscopy and X-Ray Diffraction," *Engineering, Technology & Applied Science Research*, vol. 10, no. 3, pp. 5845–5850, Jun. 2020, https://doi.org/10.48084/etasr.3288.

[27] M. T. Lakhiar, S. Sohu, I. A. Bhatti, N. Bhatti, S. A. Abbasi, and M. Tarique, "Flexural Performance of Concrete Reinforced by Plastic Fibers," *Engineering, Technology & Applied Science Research*, vol. 8, no. 3, pp. 3041–3043, Jun. 2018, https://doi.org/10.48084/etasr.2084.